Electronic Supplementary Information

Polyethyleneimine functionalized platinum superstructures: Enhancing hydrogen evolution performance by morphological and interfacial control

Guang-Rui Xu,[‡a] Juan Bai,[‡a] Jia-Xing Jiang,[a] Jong-Min Lee*[b] and Yu Chen*[a]

[a]Key Laboratory of Macromolecular Science of Shaanxi Province, Key Laboratory of Applied Surface and Colloid Chemistry (MOE), Shaanxi Key Laboratory for Advanced Energy Devices, School of Materials Science and Engineering, Shaanxi Normal University, Xi'an 710062, China. Email: ndchenyu@gmail.com (Y. Chen)

[b]School of Chemical and Biomedical Engineering, Nanyang Technological University, Singapore 637459, Singapore. Email: jmlee@ntu.edu.sg (J. M. Lee)

‡These authors contributed equally to this work.

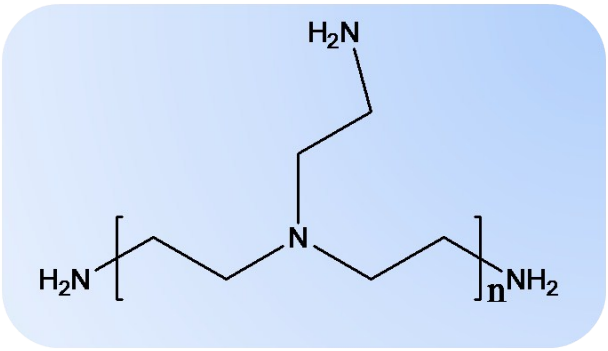

Scheme S1 Molecular structure of PEI.

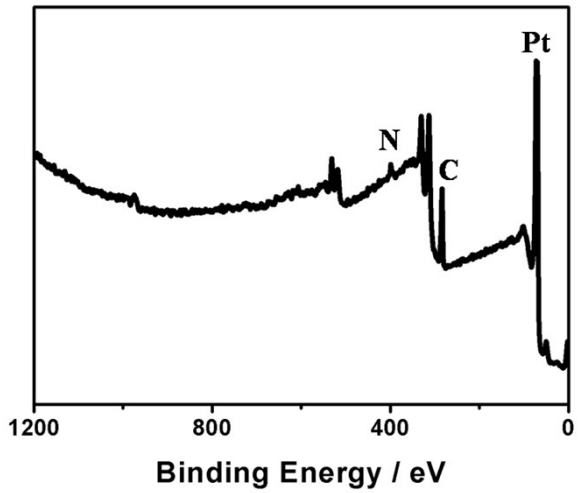

Fig. S1. The XPS scan of Pt-SSs@PEI.

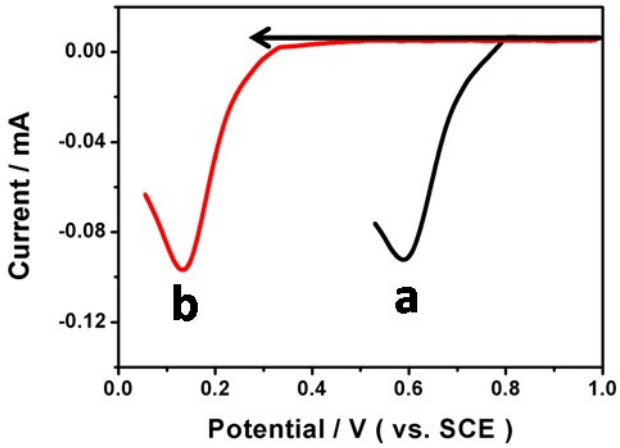

Fig. S2. LSV curves of (a) the single-component K_2PtCl_4 solution and (b) the mixture solution of K_2PtCl_4 + PEI in 0.1 M KCl electrolyte (pH 2.0) at the glassy carbon at 100 mV s^{-1}.

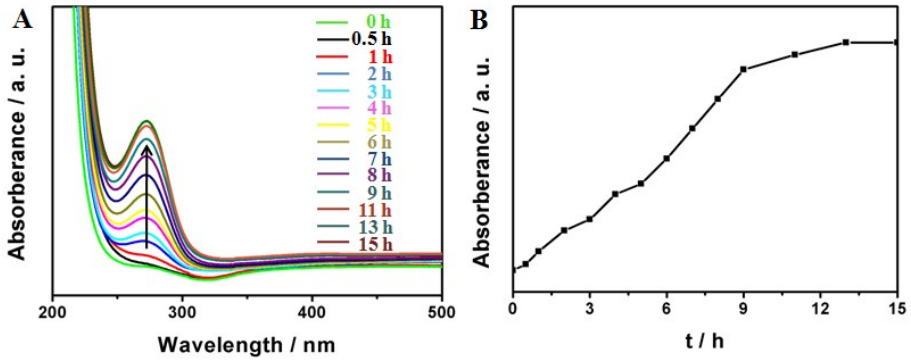

Fig. S3. (A) Time-dependent UV−vis absorption spectra of the mixture solution of K_2PtCl_4 + PEI after addition of $N_2H_4 \cdot H_2O$ and (B) the corresponding plot of the absorbance intensity of Pt nanocrystals at 260 nm as a function of time.

Fig. S4. Digital photographs of the reaction intermediates collected at (A) 0, (B) 3, (C) 6, (D) 9, (E) 12, and (F) 15 h, respectively.

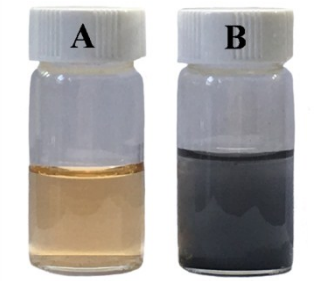

Fig. S5. The digital photographs of 9 ml 5 mM of K_2PtCl_4 aqueous solution (A) before and (B) after the addition of 1 ml of $N_2H_4 \cdot H_2O$ at 3 min.

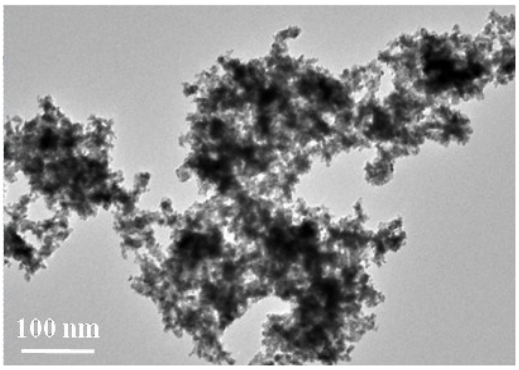

Fig. S6. TEM image of Pt aggregates without PEI.

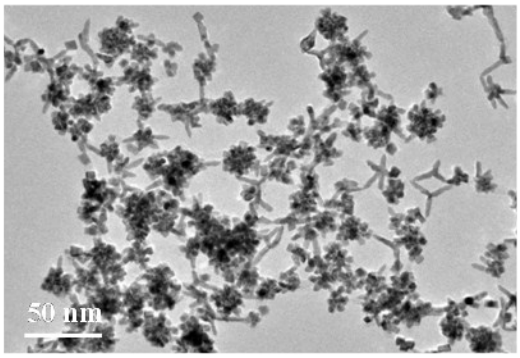

Fig. S7. TEM image of Pt aggregates by replacing PEI with polyallylamine with straight-chain structure.

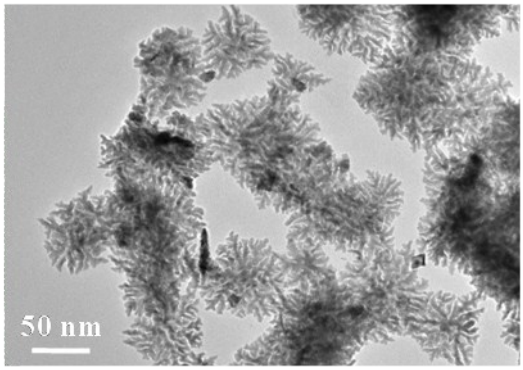

Fig. S8. TEM image of Pt-SSs@PEI after increasing reaction time to 25 h at 80 °C.

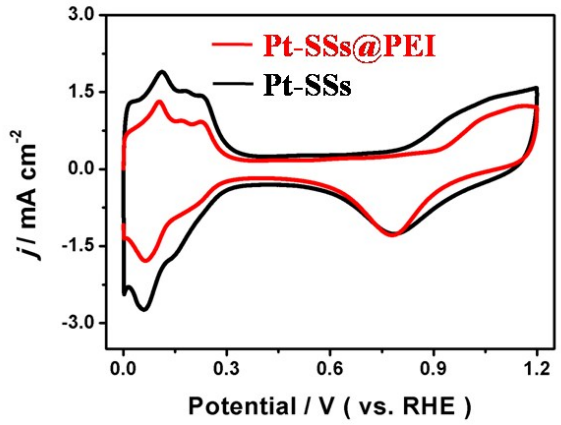

Fig. S9. CV curves of Pt-SSs@PEI and Pt-SSs in a N_2-saturated 0.5 M H_2SO_4 solution at 50 mV s^{-1}.

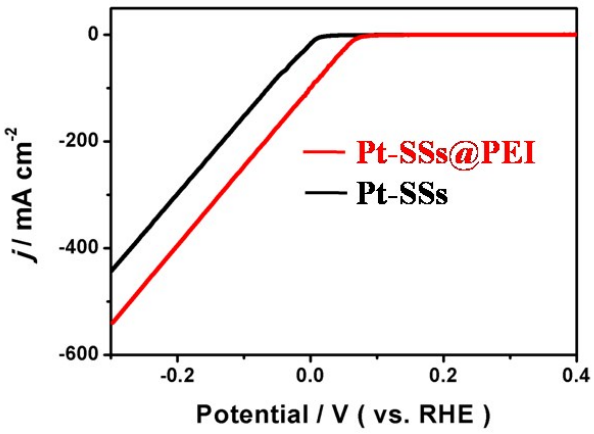

Fig. S10. LSV curves of Pt-SSs@PEI and Pt-SSs in a N_2-saturated 0.5 M H_2SO_4 solution at 2 mV s^{-1} and rotating rate of 1600 rpm.

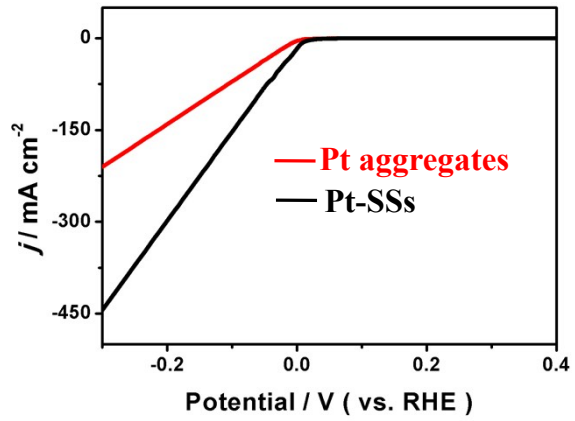

Fig. S11. LSV curves of Pt aggregates and Pt-SSs without PEI in a N_2-saturated 0.5 M H_2SO_4 solution at 2 mV s^{-1} and rotating rate of 1600 rpm.

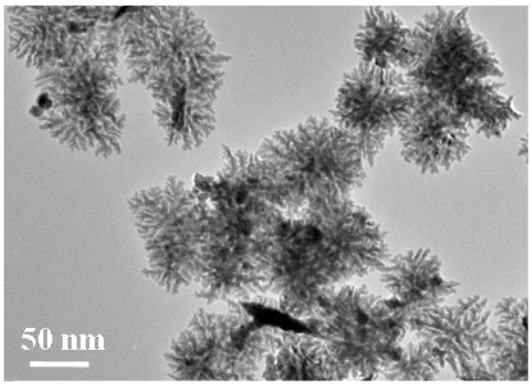

Fig. S12. TEM image of Pt-SSs@PEI after 10, 000 CV cycling.

Table S1 The E_{onset} value of recently reported various Pt-based nanostructures for the HER.

Catalysts	Electrolyte	E_{onset} value (vs. RHE)	Ref
Pt-SSs@PEI	0.5 M H_2SO_4	. +64.6 mV	This work
Pt–Au alloy	0.5 M H_2SO_4	. −200 mV	Ref. 51
Single-walled carbon nanotubes with pseudo-atomic-scale platinum	0.5 M H_2SO_4	. −10 mV	Ref. 52
Pt nanoparticles on N-doped carbon	0.5 M H_2SO	. −2 mV	Ref. 53
Pt confined in a calixarene-based {Ni24} coordination cage	0.5 M H_2SO	. −40 mV	Ref. 42
Pt single-atom	0.5 M H_2SO	. −40 mV	Ref. 6
Pt–Ni nanowires	0.5 M H_2SO	. −15 mV	Ref. 43
Pt nanoparticles on carbon nanofibers	0.5 M H_2SO	. −50 mV	Ref. 44
$Pt_{81}Fe_{29}Co_6$ nanoparticles	0.5 M H_2SO	. −10 mV	Ref. 10
Pt/N-doped carbon	0.5 M H_2SO_4	. −5 mV	Ref. 45
Pt on Pd nanocubes	0.5 M H_2SO_4	. −25 mV	Ref. 46
PtCuNi alloys	0.5 M H_2SO_4	. −60 mV	Ref. 47
PtNi alloy	0.1 M KOH	. −65 mV	Ref. 48
PtNi /NiS nanowires	1 M KOH	. −50 mV	Ref. 3
Pt-$Ni(OH)_2$ nanocomposites	0.1 M KOH	. −200 mV	Ref. 49
Ni_3N/Pt composite	1 M KOH	. −40 mV	Ref. 50